Supplementary Materials for

The fitness landscape of a tRNA gene

Chuan Li, Wenfeng Qian, Calum J. Maclean, and Jianzhi Zhang

correspondence to: jianzhi@umich.edu

This PDF file includes:

Materials and Methods
Figures S1 to S11
Tables S1 to S4

Materials and Methods

Media

Standard YPD (1% yeast extract, 2% peptone, 2% glucose) and YPG (1% yeast extract, 2% peptone, 3% glycerol) media were used as indicated. These two media differ in the carbon source, with YPD providing glucose as a fermentable carbon source and YPG providing glycerol as a non-fermentable carbon source. Complete Supplement Media (CSM) used contained 0.017% yeast nitrogen base without amino acids, 0.5% ammonium sulfate, 2% glucose, with addition of appropriate CSM drop-out mix as outlined by the manufacturer (Clontech).

Assessing the fitness effects of $tRNA^{Arg}_{CCU}$ gene deletion across environments

Two different environments are needed in this experiment. The first is a permissive environment, for collection of transformants, in which growth rate differences among tRNA variant-carrying cells are minimized in order to maximize equal representation in the initial tRNA gene variant pool. A second selective environment is then required where the fitness variation among cells carrying different tRNA gene variants is maximized, allowing a fitness landscape to be determined.

To identify these two environments, we first replaced the single-copy wild-type $tRNA^{Arg}_{CCU}$ gene (standard gene name *HSX1*) with *LEU2* in the haploid strain BY4742 (*MATα; his3Δ 1; leu2Δ 0; lys2Δ 0; ura3Δ 0; hsx1::LEU2*) (**Fig. S1**), followed by confirmation by Sanger sequencing. Growth curves for the wild-type strain and the strain lacking the $tRNA^{Arg}_{CCU}$ gene were then determined by optical density at 600 nm every 15 minutes for 24 hours using a Synergy H1 Microplate Reader across multiple environments, consisting of combinations of two media (YPD and YPG) and three temperatures (30, 35 and 37°C) (**Fig. S2**). The highest slope of the growth curve during the log phase was calculated for each growth curve following a previously established method (*23*). For the reasons outlined in the previous paragraph, YPD at room temperature was chosen as the condition for transformation, while YPD at 37°C was chosen as the condition for fitness landscape determination.

Chemical synthesis of yeast tRNA gene variants

The yeast $tRNA^{Arg}_{CCU}$ gene was chemically synthesized by IDT (https://www.idtdna.com/site). IDT cannot synthesize oligonucleotides longer than 100 nucleotides with sequence variations that require manual mixing of nucleotides. With this limit of the total length and the need for constant regions at the two ends of the oligonucleotides for polymerase chain reaction (PCR), 69 variable sites are allowed. That is, the first nucleotide and last two nucleotides (counting from the 5' end) of the 72-nucleotide gene were invariant and synthesized according to the wild-type sequence. At each of the 69 variable sites, the probability of incorporating the wild-type nucleotide was set at 0.97, while the probability of incorporating each of the other three nucleotides was 0.01. The DNA sequence synthesized is TTCAACCAAGTTGGttccgtttgcgtaatggtaacgcgtctccctcctaaggagaagactgcgggttcgagtcccgtacggaaCGTTGATTATTTTTTTT, where capital letters indicate the nucleotides at invariant sites while lower-case letters indicate the nucleotides with 97% probability at

variable sites. The underlined region corresponds to the tRNA gene, whereas the flanking non-underlined regions are used for fusion PCR and homologous recombination (**Fig. S1**). Using 97% wild-type nucleotides at each variable position maximizes the fraction of variants carrying two mutations, facilitating the study of pairwise epistasis. In the pool of tRNA gene variants synthesized, the fractions of molecules with 0, 1, 2, 3, 4 and >4 mutations are expected to be 12%, 26%, 27%, 19%, 10%, and 6%, respectively, while the possible numbers of variants with 0, 1, 2, 3, and 4 mutations are 1, 207, 2.1×10^4, 1.4×10^6, and 7.0×10^7, respectively. Sanger sequencing of 24 randomly picked variants confirmed that the synthesis was as expected and contained no indel. The mutation rate was estimated to be 3.2±0.29%, not significantly different from the expected value of 3%, and different base changes were roughly equally frequent.

Construction of the tRNA gene variant strain pool

The pool of synthesized single-stranded oligonucleotides were amplified by PCR and then fused with the *URA3* marker gene by PCR (**Fig. S1**). High fidelity AccuPrime™ *Pfx* DNA polymerase was used in all PCR reactions. The tRNA gene deletion strain (*MATα; his3Δ 1; leu2Δ 0; lys2Δ 0; ura3Δ 0; hsx1::LEU2*) was then transformed with the *tRNA-URA3* variant cassette to integrate a single tRNA gene variant and to simultaneously remove *LEU2* at the native tRNA gene locus. Over 100,000 colonies were collected from CSM minus uracil plates by washing with sterile water. The large number of colonies collected ensured the inclusion of a large number of tRNA gene variants. Pooled variants were stored in 20% glycerol at -80°C.

Competition

A frozen sample of cells carrying tRNA gene variants was removed from storage at -80°C and allowed to revive at 30°C in YPD for 3 hours. Six replicate competitions were then started by dilution of this common starter population into six 50 ml Falcon tubes, each containing 25 ml of YPD at 37°C at an initial OD660 = 0.1. Each culture was maintained at 250 RPM in a shaking incubator and diluted to OD660 = 0.1 through transfer to fresh 25 ml of YPD media every 12 hours, at which time population aliquots were also frozen in 20% glycerol at -80°C. The competitions lasted for 24 hours.

Library preparation, Illumina sequencing, and read mapping

DNA was extracted from thawed population aliquots of interest. We amplified the tRNA gene from cell populations using two rounds of PCR to ensure that only those tRNA gene variants that are inserted at the native location were amplified (**Fig. S1**; **Table S1**). Two technical repeats of the starting population before competition (T_0) and six biological replicates from the populations after 24 hours in competition (T_{24}) were subjected to 100-nucleotide paired-end Illumina sequencing. Paired reads for the tRNA gene sequence are required to be identical to be counted. Read counts are combined across technical repeats or biological replicates in subsequent analyses unless otherwise noted. To ensure relative accuracy in fitness estimation, 65,537 genotypes with a total of at least 100 reads in the two technical repeats at T_0 were analyzed.

PCR and sequencing errors

The error rate for Illumina sequencing is 3×10^{-4} per site per read (http://www.illumina.com/documents/products/technotes/technote_Q-Scores.pdf). Thus, due to sequencing error, a genotype is expected to lose $U = [1-(1-3\times10^{-4})^{2\times69}]M_0$ read pairs, where M_0 is the true number of read pairs of the genotype. Because the fractional loss $U/M_0 = 0.04$ is a constant for all genotypes including the wild-type in each sample, the loss of reads due to sequencing error does not affect fitness estimation. Sequencing error also causes the genotype to gain on average $V = (3\times10^{-4}/3)^2 M_1 = 10^{-8}M_1$ read pairs, where M_1 is the total number of reads for all neighbors of the focal genotype (i.e., the genotypes that differ from the focal genotype by one nucleotide). Thus, the fractional gain of read pairs for the genotype is expected to be $V/M_0 = 10^{-8}M_1/M_0$, which has virtually no impact on fitness estimation in our study. For instance, at T_0, for the wild-type, M_1/M_0 is expected to be ~2; for an N1 genotype, M_1/M_0 is expected to be 99; for an N2 genotype, M_1/M_0 is expected to be $2\times99 = 198$; and so on. Hence, the fractional gain of read pairs is $<10^{-5}$ for genotypes with no more than 10 mutations.

We similarly estimated the impact of PCR error. AccuPrime™ *Pfx* DNA polymerase used in PCR has a very low error rate of 2.9×10^{-6} per nucleotide incorporated (https://tools.thermofisher.com/content/sfs/brochures/711-021834%20AccuPrime%20Brochu.pdf). Each of the two PCRs used in sequencing library preparation had 30 cycles. Because later cycles are inefficient, we considered effectively 50 cycles total for the two PCRs. Thus, due to PCR error, a genotype is expected to lose $U = (2.9\times10^{-6}\times69\times50)\ M_0$ molecules, where M_0 is the true number of DNA molecules of the genotype, 69 is the sequence length in nucleotides, and 50 is the total number of PCR cycles. Because the fractional loss $U/M_0 = 0.01$ is a constant for all genotypes in each sample, the loss of molecules due to PCR error does not affect fitness estimation. Sequencing error also causes the genotype to gain on average $V = 2.9\times10^{-6}\times50/3\ M_1 = 4.8\times10^{-5}M_1$ molecules, where M_1 is the total number of molecules for all neighbors of the focal genotype. Thus, the fractional gain of molecules for the genotype is expected to be $V/M_0 = 4.8\times10^{-5}M_1/M_0$, which has little impact on fitness estimation in our study. As mentioned, at T_0, for the wild-type, M_1/M_0 is expected to be ~2; for an N1 genotype, M_1/M_0 is expected to be 99; for an N2 genotype, M_1/M_0 is expected to be $2\times99 = 198$; and so on. Hence, the fractional gain in the number of molecules is < 0.024 for genotypes with no more than 5 mutations.

To independently validate the above calculations that are based on the published sequencing and PCR error rates, we estimated the upper bound rate of error caused by PCR and sequencing. It is very unlikely for any N1 genotype at T_{24} to have all of its reads arising from its neighbors by PCR and sequencing errors. Thus, by assuming that all these reads are from errors, we can estimate the upper bound error rate. We calculated the frequency of each N1 genotype in each replicate in T_{24} and identified the smallest frequency among the total of $207\times6=1242$ frequencies and the corresponding genotype. We then divided the total number of read pairs for this genotype in the other five replicates by the total number of read pairs for its neighbors in these five replicates. The result, 5.0×10^{-5}, is an upper bound estimate of the probability that a genotype "mutates" to a specific neighbor, or V defined earlier. Interestingly, this upper bound estimate of V from the sum of PCR error and the much lower sequencing error is virtually identical to that calculated based on the published PCR error rate. Together, these analyses suggest that PCR and sequencing errors have minimal impacts on our fitness estimation.

Number of generations of competition

During competition, cell populations were diluted every 12 hours, with OD660 recorded before and after dilution. From the sequencing results, we calculated the frequency of the wild-type at the beginning of the competition (F_0) and at 24 hours in competition (F_{24}). The number of wild-type generations for the 24 hours is then $G = \log_2(dgF_{24}/F_0) = 11.5$, where d is the dilution factor and g is the ratio between the cell number calculated from OD660 (*23*) at 24 hours and that at the beginning of the competition.

Estimating relative fitness from read frequency changes

Using a method previously designed for the fitness estimation of gene deletion strains (Bar-seq) (*24*), we estimated the relative fitness of each strain by using the 72-nucleotide tRNA sequence that it carries as the barcode to directly determine its abundance within the population at each time point. The per generation Darwinian fitness of a variant relative to the wild-type is

$$\text{Fitness} = \left(\frac{\#\text{ of reads for the variant at } T_{24} / \#\text{ of reads for the variant at } T_0}{\#\text{ of reads for the wild-type at } T_{24} / \#\text{ of reads for the wild-type at } T_0} \right)^{1/G}$$, where G =11.5 is the number of wild-type generations in 24 hours. By definition, the wild-type fitness is 1. If the read number drops to 0 in all six replicates or if fitness drops under 0.5, fitness was assigned to be 0.5, representing no cell division for this variant. There are six biological replicates, and we used a *t*-test to examine if the fitness of a variant is significantly different from 1 at a nominal *P* value of 5%. Comparison of read frequencies obtained from populations before and after competition corrects for frequency differences among genotypes in the starting population and potential biases in variant-specific PCR amplification efficiency, sequencing library preparation efficiency, as well as any Illumina sequencing efficiency and accuracy differences that may exist.

Because the tRNA gene deletion strain can grow (**Fig. S2**), the gene is nonessential. However, the deletion strain was not in the pool of genotypes that underwent Bar-seq, so we could not directly compare a genotype with the deletion strain to examine the potential existence of dominant negative effects. For a genotype to have a computed fitness <0.5, its frequency relative to the wild-type (w) must decrease by at least $2^{11.5}$= 2896 folds from T_0 to T_{24}. For an average N2 mutant, the expected w at T_0 is 10^{-4}. So, the expected w is $<3\times10^{-8}$ in T_{24} if its fitness is <0.5. Given the bottleneck population size of $\sim3\times10^7$ (at dilution) and final population size of $\sim1.7\times10^9$ in the competition, such a small w means that the corresponding cell number is very low. Thus, the fate of the genotype depends largely on genetic drift. In other words, the formula for estimating mutant fitness in the previous paragraph, which ignores genetic drift, would not work well. Given the known function of tRNAs, the most likely reason for potential dominant negative effects would be anticodon mutations. Yet, most mutants with anticodon mutations have fitness >0.5 (**Table S3**). Thus, dominant negative effects probably do not exist here, but further studies are certainly required to confirm this point.

Fitness estimation from growth curves

In order to verify our *en masse* fitness estimates, we isolated 55 strains from the variant pool with distinct tRNA gene sequences based on Sanger sequencing. The

growth rates of the 55 strains were measured using Bioscreen C OD reader at 37°C in YPD. Cells were grown at room temperature overnight until saturation, and then diluted by a factor of 50 to roughly OD600 = 0.1. OD measurements at wide band (450-580 nm) were taken every 20 minutes for 48 hours. Proliferation efficiency and maximum growth rate were calculated following standard procedures from measurement 10 to 72 (*25*). Two biological replications in fitness measurement were performed per genotype.

Fitness estimation by pairwise competition

To further confirm our *en masse* fitness estimates, we performed pairwise competition assays of the 55 strains against a fluorescent reference strain. The reference strain, YCM2644 (*MATα; his3Δ 1; leu2Δ 0; lys2Δ 0; URA3; ho::TDH3p-VenusYFP-HygMX4*), was constructed by replacing the *HO* gene in a strain that carries the native tRNA gene and *URA3* with a cassette comprised of a yellow florescent protein (YFP) gene and a hygromycin resistance gene. We also competed between the reference stain and one of the constructed variant strains that happens to carry the wild-type tRNA gene (referred to as the wild-type variant). The competition procedure followed that in the main experiment. Samples were collected at 0 and 24 hours, and the fitness of each variant strain relative to that of the wild-type variant was calculated following an established protocol (*20*). Three biological replications in fitness measurement were performed.

Comparing growth rates across multiple environments

We measured the growth rates of the aforementioned 55 strains using Bioscreen C OD reader in four environments at 30°C: YPD, YPD with 7% EtOH, YPD with 3% DMSO, and YPD with 0.85M NaCl. Cells were grown at room temperature overnight until saturation, and then diluted by a factor of 100 to roughly OD600 = 0.1. OD measurements at wide band (450-580 nm) were taken every 20 minutes for 24 hours. Maximum growth rates were calculated as described above. Three biological replications were performed. Growth rates in these four environments and those in YPD at 37°C were compared for the 55 strains.

Phylogenetic data of the tRNA genes

From GtRNAdb (http://gtrnadb.ucsc.edu), we downloaded 1098 eukaryotic tRNA genes with anticodon CCU. A total of 416 distinct sequences were aligned using the cmalign program in the Infernal package (http://infernal.janelia.org/), which aligns tRNA sequences based on both the primary sequence and the secondary structure. The region corresponding to the 72-nucleotide segment of yeast tRNA was extracted for further analysis. To acquire a good representation of the tRNA sequence variation over evolutionary time and avoid oversampling from certain well-studied groups of organisms, we calculated the pairwise sequence distances among the tRNA genes, and randomly removed one of the two sequences with the smallest distance until the distance between any two sequences in the dataset is at least 7 nucleotides (~10%). A total of 200 sequences remained in this dataset. We also examined a subset of 23 sequences, each having at least 20 nucleotide differences from any other sequences in the subset, and obtained qualitatively similar results as those from the 200 sequences.

Estimating epistasis from fitness values

Epistasis is defined as $\varepsilon = f_{AB} - f_A f_B$, where f_{AB} is the fitness of a N2 mutant and f_A and f_B are the fitness of the two corresponding N1 mutants. ε is computed by $f_{AB} - 0.5$ when $f_A f_B < 0.5$. The overall distribution of ε is unaffected when we exclude 854 cases in which f_{AB} or $f_A f_B$ is ≤ 0.5 (**Fig. S7A**). To examine if ε differs significantly from 0, we estimated ε from each of the six biological replicates and conducted a *t*-test.

In the tRNA under study, there are 20 paired stem sites, with 1 being wobble pairing (GU) and the rest 19 being WC pairing. Pairwise epistasis is more likely to be positive when two mutations occur at paired sites than when they do not occur at paired sites. It is easy to understand why epistasis is positive when the second mutation restores pairing after the first mutation breaks it. Further, even when pairing is not restored by the second mutation, epistasis could be positive, likely because the second mutation does no more harm to pairing when the pairing has been broken by the first mutation. Nevertheless, even at paired sites, epistasis is not always positive, suggesting that base pairing is not the sole function of the nucleotides at paired sites such that the second mutation, regardless of whether it restores pairing, could do additional harm.

Sign epistasis occurs when the fitness effect of a mutation is opposite depending on the presence or absence of another mutation. That is, sign epistasis satisfies $(f_A - 1)(f_{AB}/f_B - 1) < 0$ or $(f_B - 1)(f_{AB}/f_A - 1) < 0$. Reciprocal sign epistasis satisfies $(f_A - 1)(f_{AB}/f_B - 1) < 0$ and $(f_B - 1)(f_{AB}/f_A - 1) < 0$. Statistical significance was determined as described above. In total, 160 cases of significant sign epistasis were found, 6 of which were reciprocal sign epistasis. Interestingly, 75 of the 160 cases involved T8C and 54 involved A70C, suggesting that sign epistasis is highly concentrated at a few sites. The reason why T8C and A70C are concentrated in significant sign epistasis cases is that they are the only significantly beneficial mutations in the wild-type background, but they apparently are deleterious in many N1 backgrounds. Among the 160 sign epistasis cases, 9 involve paired sites in stems, significantly more than the chance expectation ($P < 0.05$, χ^2 test). This is not unexpected, because a mutation at a stem site could either destroy or restore a base pair depending on the presence or absence of the pairing before the mutation.

We predicted the mean fitness of mutants carrying *n* mutations from the fitness of N1 mutants, under the assumption of no epistasis (red circles in **Fig. 2E**). For each mutant with *n* mutations, the predicted fitness is the product of the fitness of the constituent N1 mutants or 0.5 if the product is < 0.5. We then averaged the predicted fitness for all mutants with *n* mutations.

Varying pairwise epistasis in different genetic backgrounds

To examine whether the sign of pairwise epistasis varies depending on the genetic background, we compared the epistasis between mutations A and B in the wild-type and that in the N1 mutant carrying mutation C. Epistasis in the wild-type is calculated by $\varepsilon_{AB}|\mathrm{WT} = f_{AB} - f_A f_B$, while epistasis in the N1 mutant is calculated by $\varepsilon_{AB}|\mathrm{C} = f_{ABC}/f_C - (f_{AC}/f_C)(f_{BC}/f_C)$. The expected fitness $f_A f_B$ and $(f_{AC}/f_C)(f_{BC}/f_C)$ are set to be 0.5 if smaller than 0.5.

An alternative measure of pairwise epistasis

We also used an alternative definition of epistasis based on an additive model of the logarithm of fitness, $\varepsilon' = \ln(f_{AB}) - \ln f_A - \ln f_B$, to calculate all pairwise epistasis (**Fig. S8**), but found the general pattern unchanged.

Structural stability and fraction of correctly folded tRNA molecules

The function/fitness relevance of mutational impacts on protein structure stability is well known (*26*), and we here examine the importance of RNA structure stability to fitness. The secondary structure of the wild-type tRNA follows http://lowelab.ucsc.edu/GtRNAdb/Sacc_cere/Sacc_cere-structs.html. For each tRNA variant, a series of suboptimal secondary structures and the corresponding minimum free energy (E) were predicted from the "subopt" function in the Vienna RNA package (*27*) at 37°C. The predicted proportion of functional tRNA molecules is estimated by $P_{\text{func}} = [\sum_i (J_i e^{\frac{-E_i}{kT}})] / (\sum_i e^{\frac{-E_i}{kT}})$. Here, i refers to the ith considered secondary structure, J_i is an identity function, taking the value of 0 if the structure i is not functional and 1 if it is functional, E_i is the minimum free energy of the ith structure, $k = 0.001987$ kcal/mol/K is the Boltzmann constant, and $T = 310$ K is the absolute temperature corresponding to 37°C. We considered only those structures whose E values are smaller than 3 kcal/mol + the E value of the most stable structure for the mutant concerned. If the wild-type structure is not included within the 3 kcal/mol range, we add it (with the constraint of the mutant sequence) to the list of predicted structures, with E predicted by the energy_of_struct function of the Vienna package. A structure is considered functional when it satisfies two criteria. First, no base pairing occurs at any position of the anticodon and no mutation occurs at any position of the anticodon. Second, the distance between the structure considered and the wild-type structure does not exceed $d = 2$. The distance was calculated by the RNAdistance function in the Vienna package. We varied the parameter d between 0 and 16 and found the result qualitatively unchanged.

LOESS regression and prediction of epistasis from P_{func}

LOESS regression in R was used to summarize the relationship (and 95% confidence interval) between fitness and P_{func} for N1, N2, and N3 mutants, respectively. The span parameter α was set at 1 and all other parameters were as default. For each N2 mutant, epistasis is predicted in the following manner. First, the P_{func} of the N2 mutant is computed as described above. Second, the corresponding fitness is predicted using the LOESS curve for N2 mutants. Third, P_{func} is computed for each of the two corresponding N1 mutants. Fourth, fitness is predicted for each of the two N1 mutants from the LOESS curve for N1 mutants. Fifth, epistasis is then calculated based on the three predicted fitness values as if they are observed fitness values.

When we predicted epistasis using a single LOESS curve, the predicted epistasis is positively biased. For instance, when only the N1 LOESS curve is used, the mean predicted epistasis is 0.07. When only the N2 curve is used, the mean predicted epistasis is 0.16. When a combined LOESS curve for N1 and N2 mutants is used, the mean predicted epistasis is 0.16. We also found that epistasis in P_{func} in overall positive.

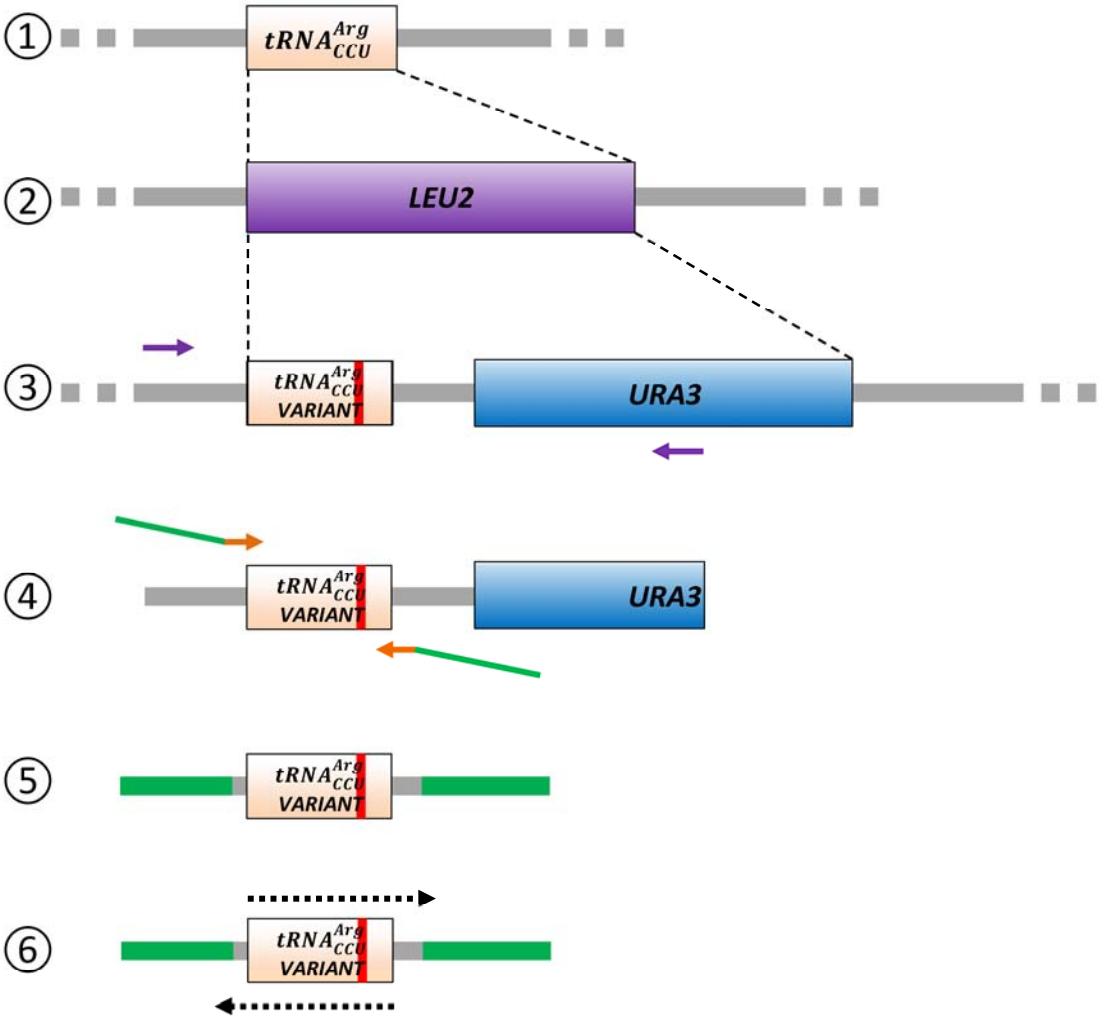

Fig. S1. Schematics of experimental procedures.
① The wild-type $tRNA^{Arg}_{CCU}$ gene at its native genomic position.
② The wild-type $tRNA^{Arg}_{CCU}$ gene is replaced with *LEU2*. The dotted black lines show the region replaced. This is the strain referred to as the $tRNA^{Arg}_{CCU}$ gene deletion strain in the paper.
③ *LEU2* is replaced with a tRNA gene cassette composed of a $tRNA^{Arg}_{CCU}$ gene variant and *URA3*.
④ Genomic region amplified by the first round of PCR with the purple primer pair shown in ③. The purple primer pair shown in ③ only amplifies tRNA gene cassettes that are located at the correct genomic position.
⑤ tRNA gene variant amplified from ④ using the orange primer pair shown in ④. Adapters for Illumina sequencing are shown by green lines and are part of the primers.
⑥ The tRNA gene variant is sequenced using 100-nucleotide paired-end Illumina sequencing, indicated by black dotted arrows.

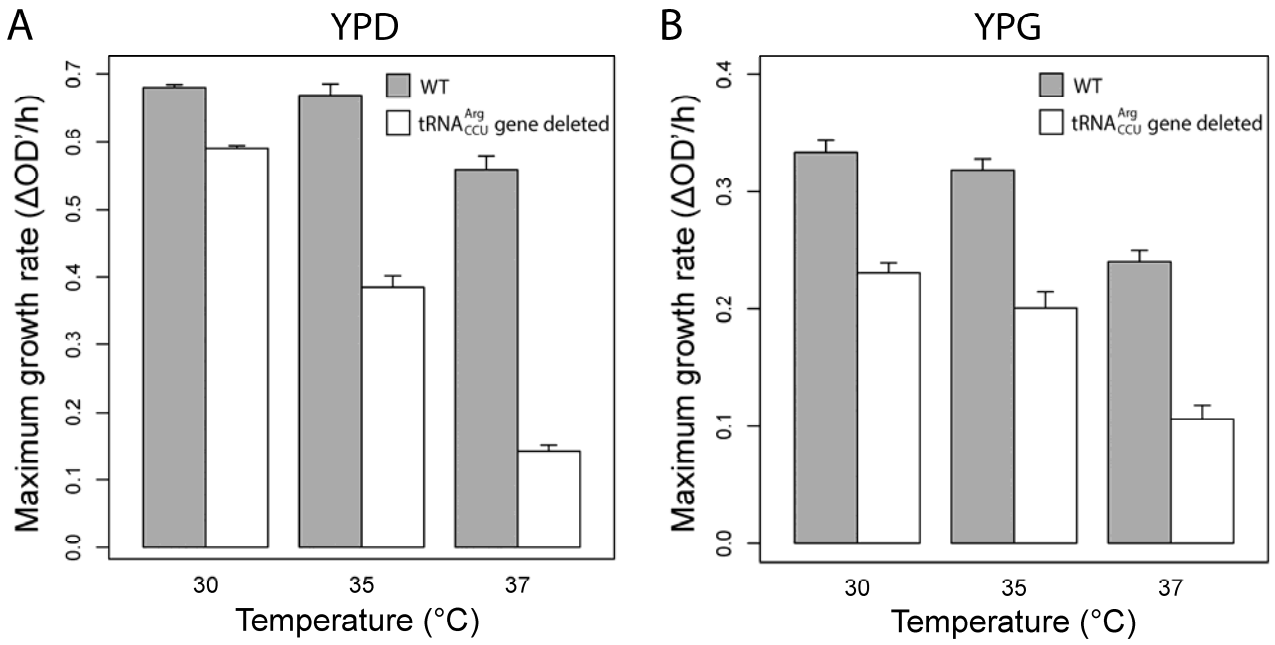

Fig. S2. Maximum growth rates of the yeast wild-type strain (gray bars) and $tRNA^{Arg}_{CCU}$ gene deletion strain (white bars) in two media at three temperatures. (**A**) Mitotic growth rates in the fermentable medium YPD. (**B**) Mitotic growth rates in the non-fermentable medium YPG. Growth rates are measured by the maximum increase in OD' per hour in mid-log phase. OD', converted from optical density (OD) at 600 nm by the formula $OD+0.8324\times OD^3$, is approximately proportional to cell density.

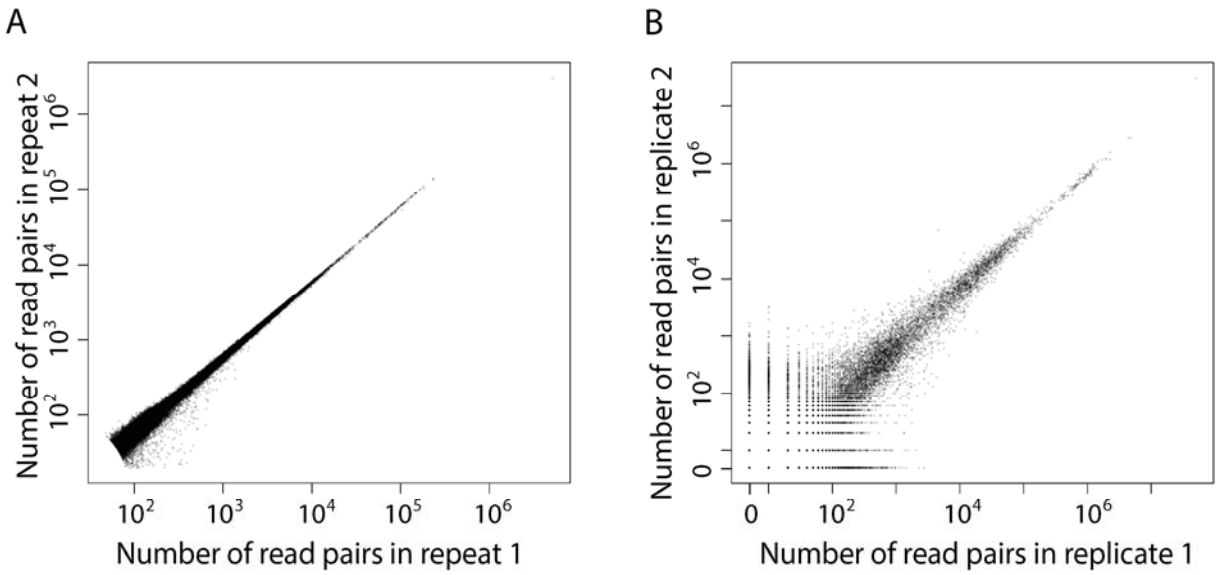

Fig. S3. Numbers of read pairs across genotypes are highly correlated between technical repeats and between biological replicates. (**A**) Comparison in read pair number between two technical repeats at T_0 across genotypes. Each dot represents a genotype and only those genotypes with a total of ≥100 read pairs are considered. Pearson's correlation coefficient $r = 0.99997$. (**B**) Comparison in read pair number between biological replicates 1 and 2 at T_{24} across genotypes. Each dot represents a genotype and only those genotypes with a total of ≥100 read pairs at T_0 are considered. Pearson's correlation coefficient $r = 0.9997$. The mean $r = 0.9987$ for the 15 pairs of biological replicates.

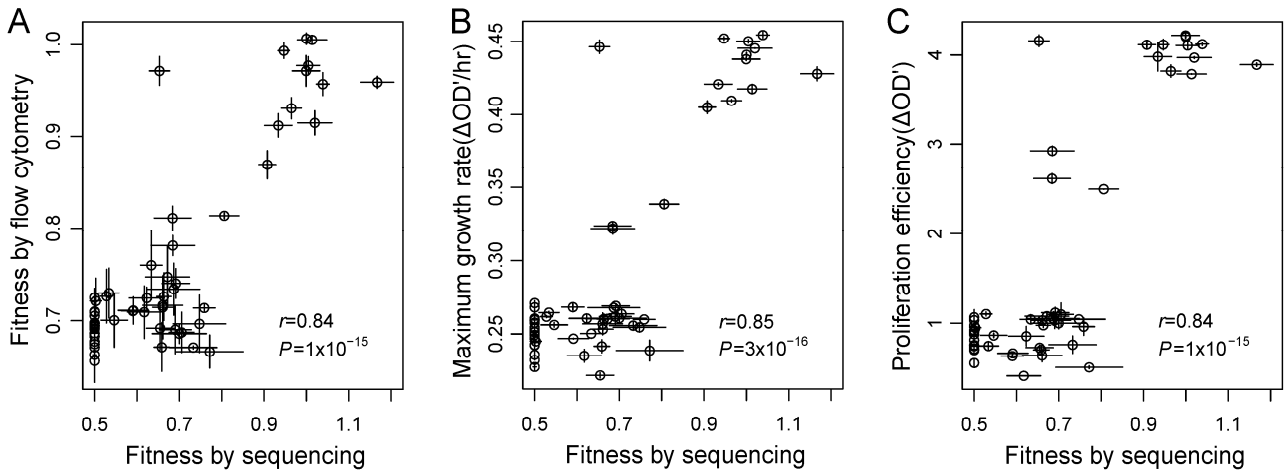

Fig. S4. Comparison of three fitness estimation methods for 55 strains carrying different tRNA variants. For the sequencing method, fitness values shown are per generation fitness relative to the wild-type. For the flow cytometry method, fitness is measured by pairwise competition followed by flow cytometry, and the values shown are per generation fitness relative to the wild-type. For the growth curve method, fitness is measured by either the maximum growth rate in mid-log phase (ΔOD'/hr) or proliferation efficiency (OD' change in the first 48 hours of growth). OD', converted from optical density (OD) by the formula $OD+0.8324\times OD^3$, is approximately proportional to cell density. (**A**) Fitness estimated by sequencing is correlated with that estimated by flow cytometry. (**B**) Fitness estimated by sequencing is correlated with that estimated by maximum growth rate. (**C**) Fitness estimated by sequencing is correlated with that estimated by proliferation efficiency. Error bars show one standard error.

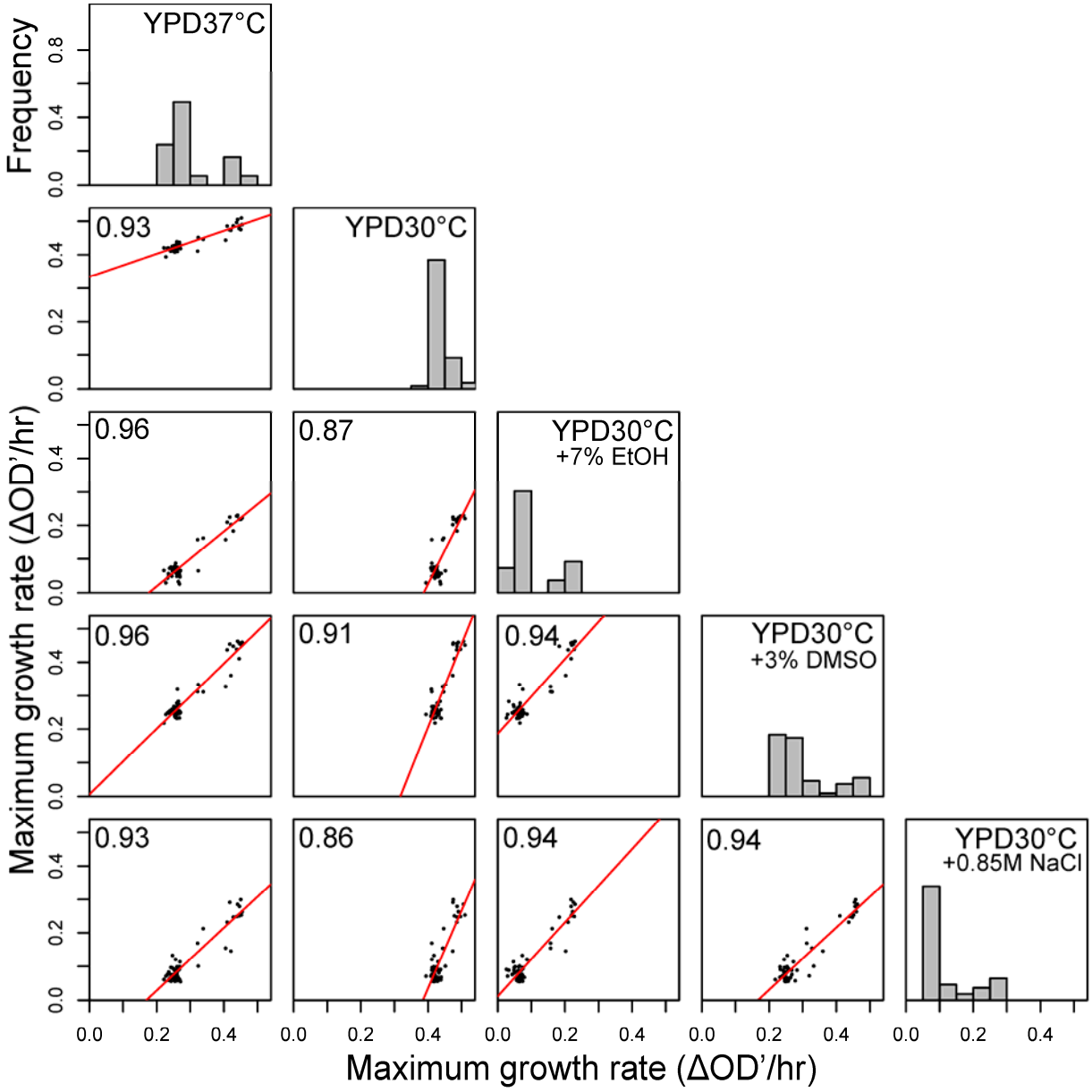

Fig. S5. Correlations of maximum growth rates of 55 strains carrying different tRNA variants among five different environments. Environments used and the frequency distribution of maximum growth rates in the environments are shown in the diagonal panels. In lower left panels are maximum growth rates in each environment plotted against those in each of the other four environments, along with Pearson's correlation coefficients and red linear regression lines.

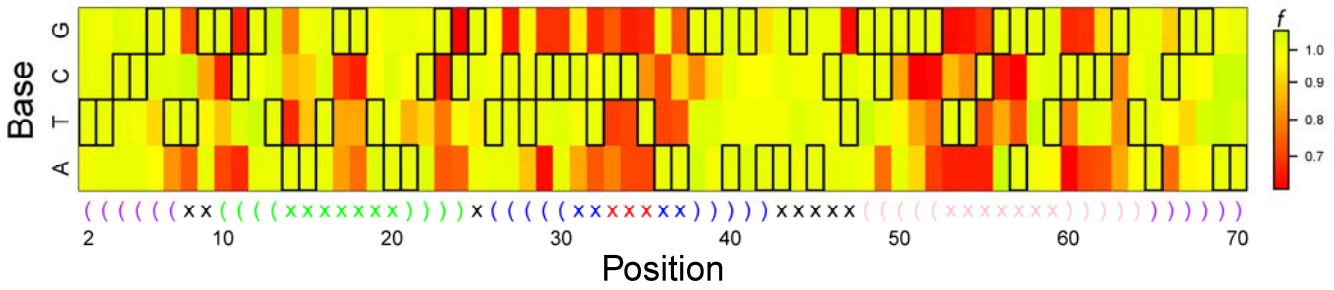

Fig. S6. Heat map showing the fitness of all N1 mutants. At each site, the wild-type nucleotide is boxed. The tRNA secondary structure is plotted linearly with parentheses showing sites in stems and crosses showing sites in loops; the same color is used for sites in the same loop or stem. The anticodon is shown by the three red crosses.

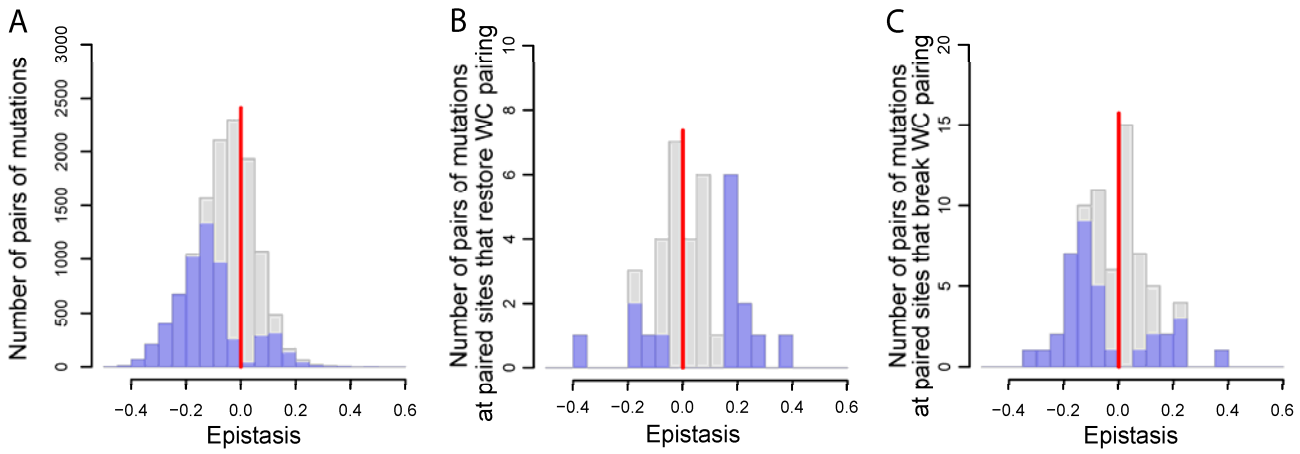

Fig. S7. Distribution of epistasis between mutations after the removal of all 854 cases with observed or expected fitness reaching the lower limit of 0.5. (**A**) Frequency distributions of pairwise epistasis (gray) and statistically significant pairwise epistasis (blue) among 12,475 pairs of point mutations studied. (**B**) Frequency distributions of epistasis (gray) and statistically significant epistasis (blue) between pairs of mutations that convert a Watson-Crick (WC) base pair to another WC pair. (**C**) Frequency distributions of epistasis (gray) and statistically significant epistasis (blue) between pairs of mutations that break a WC pair. The vertical red line shows $\varepsilon = 0$. Median ε is significantly greater in (B) and (C) than in (A) when all epistasis cases ($P = 3\times10^{-5}$ and 0.01, respectively; Mann-Whitney U test) or only significant epistasis cases ($P = 3\times10^{-4}$ and 0.02, respectively) are considered. Median ε is significantly greater in (C) than in (B) when all epistasis cases ($P = 0.049$) or only significant epistasis cases ($P = 0.043$) are considered.

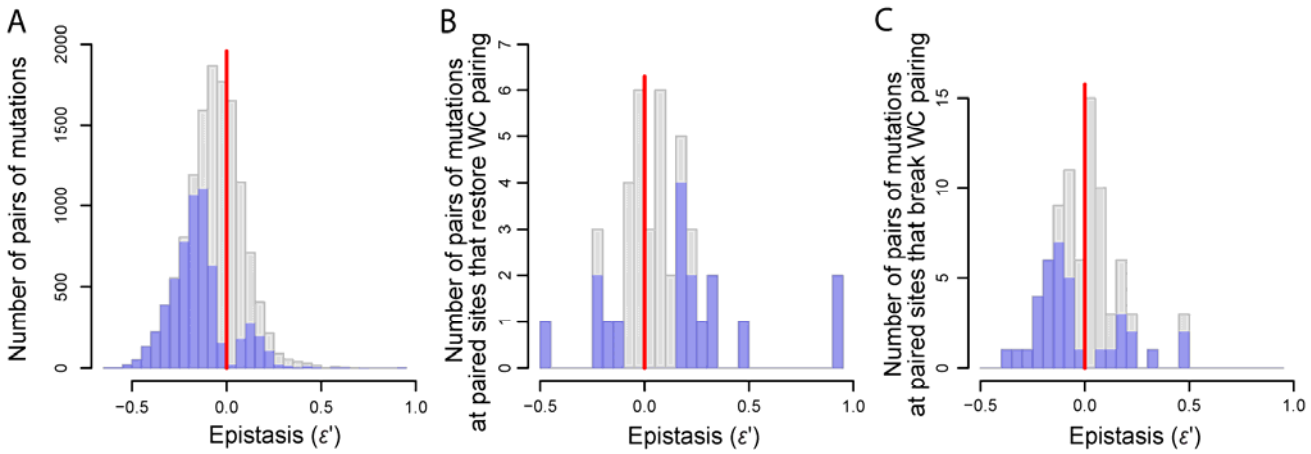

Fig. S8. Distribution of pairwise epistasis $\varepsilon' = \ln(f_{AB}) - \ln f_A - \ln f_B$. (**A**) Frequency distributions of pairwise epistasis (gray) and statistically significant pairwise epistasis (blue) among all 12,985 pairs of point mutations studied. (**B**) Frequency distributions of epistasis (gray) and statistically significant epistasis (blue) between pairs of mutations that convert a Watson-Crick (WC) base pair to another WC pair. (**C**) Frequency distributions of epistasis (gray) and statistically significant epistasis (blue) between pairs of mutations that break a WC pair.

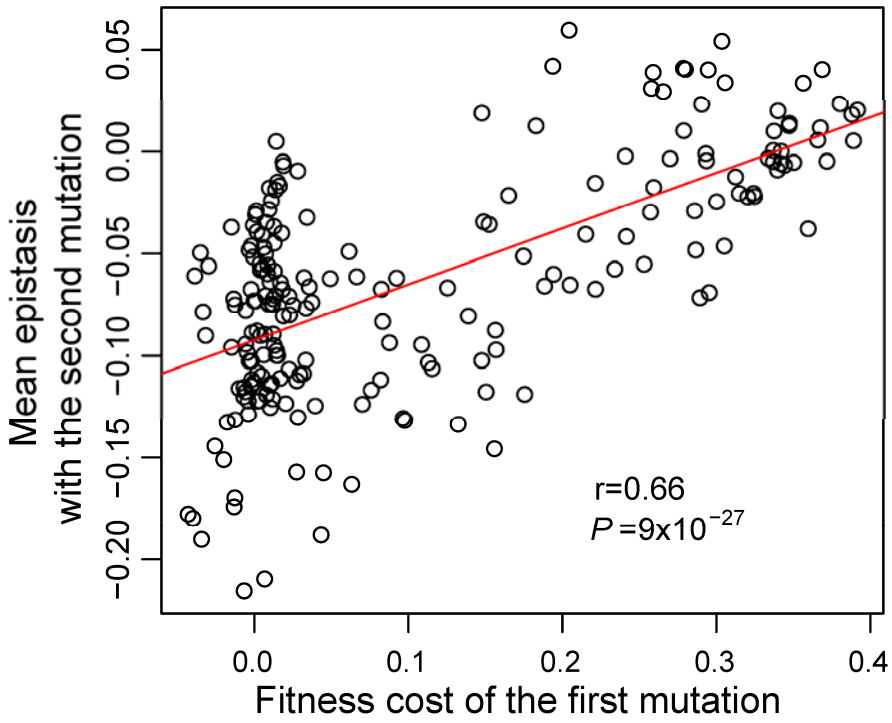

Fig. S9. Correlation between the fitness cost of the first mutation and the mean epistasis with the second mutation, after the removal of N2 mutants whose expected or observed fitness is ≤ 0.5. Red line shows the linear regression.

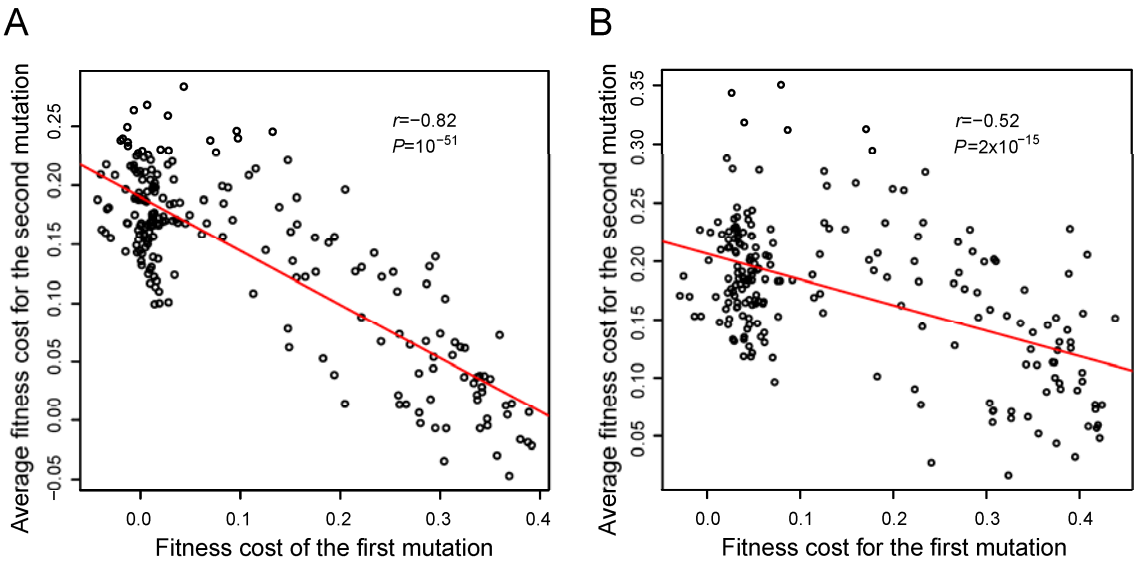

Fig. S10. Negative correlation between the fitness cost of the first mutation and the mean fitness cost of the second mutation is not artifactual. (**A**) Correlation between the fitness cost of the first mutation and the mean fitness cost of the second mutation, after the removal of all N2 mutants whose expected or observed fitness is ≤ 0.5. Red line shows the linear regression. The fitness cost of the first mutation is calculated by 1-f_A, where f_A is the fitness of a N1 mutant carrying the A mutation. The mean fitness cost of the second mutation, given the first mutation A, is calculated by 1- (mean f_{AB})/f_A, where the subscript AB refers to a genotype carrying the A mutation as well as another mutation (including the reversion of the A mutation) and f_{AB} is the average fitness of all such genotypes. (**B**) Correlation between the fitness cost of the first mutation and the mean fitness cost of the second mutation, where the x-axis and y-axis are based on fitness data from different biological replicates. Because measurement errors of f_A could lead to an artefactual negative correlation between the estimated fitness costs of the first and second mutations, we used three biological replicates to estimate f_A for the x-axis and used the other three biological replicates to estimate f_{AB} and f_A for computing the y-axis value, thus removing such potential artifacts. All 20 possible combinations of such sampling were used to calculate the correlation, which ranges from -0.51 to -0.76, with a mean of -0.61. The slope ranges from -0.397 to -0.220, with a mean of -0.293.

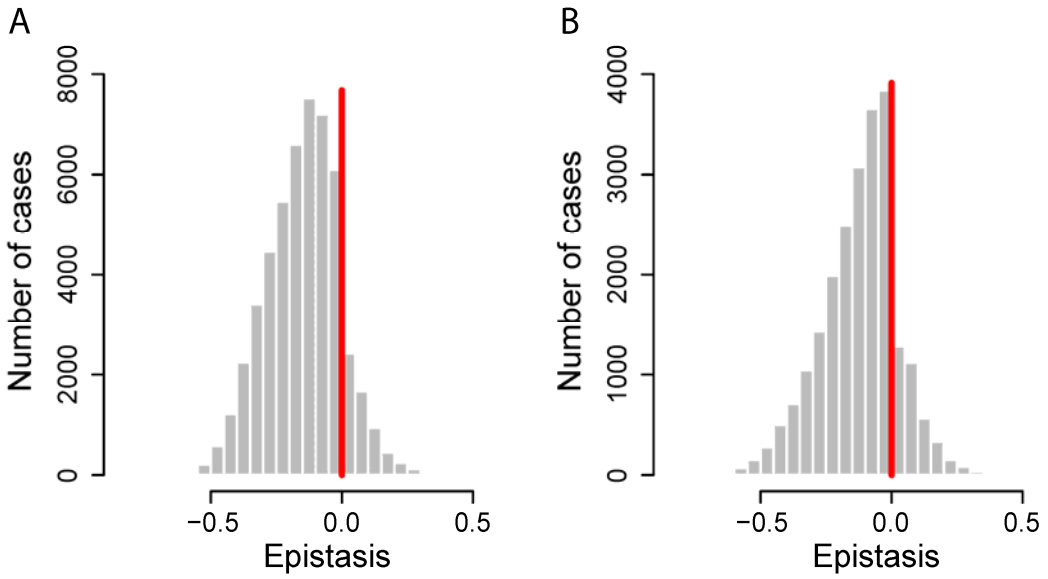

Fig. S11. Frequency distributions of pairwise epistasis involving more than two sites. (**A**) Frequency distribution of epistasis between mutations AB and mutation C, defined as $\varepsilon = f_{ABC} - f_{AB}f_C$, is overall negatively biased. 6,234 cases with epistasis = 0 (both expected and observed fitness = 0.5) are not shown. (**B**) Epistasis between mutations AB and mutations CD, defined as $\varepsilon = f_{ABCD} - f_{AB}f_{CD}$, is overall negatively biased. 9,343 cases with epistasis = 0 (both expected and observed fitness = 0.5) are not shown. Here A, B, C, and D refer to four point mutations, relative to the wild-type. The red vertical lines show zero epistasis.

Table S1. Primers used

Purpose of the primers	Forward primer (5'-3')	Reverse primer (5'-3')
Replacing the endogenous $tRNA^{Arg}_{CCU}$ gene with *LEU2*	TCGTAATAATATTACTATGCAAC TTAGGTACCTCATATTTCTTAGA GTTCAACCAAGTTGAAGAGTTC GAATCTCTTAGCAACCA	ATATGAACCTTCAACTAGTTAT TACCACTGTGGCACTCTTTCTG CGGTAAGATTATCTCACTCCAT CAAATGGTCAGGTCATTGA
Amplifying the chemically synthesized $tRNA^{Arg}_{CCU}$ gene variants	CGAAGTTTATTCATTCAATTTGA AGTGCTTCGTAATAATATTACTA TGCAACTTAGGTACCTCATATTT CTTAGAGTTCAACCAAGTTGG	TCGCAAGGTAATATCGTCTGA ATTTTTTCTATAAAGAAACGAA AAAAAAAAAATAATCAACG
Amplifying *URA3*	TTGATTATTTTTTTTTTTTCGTTT CTTTATAGAAAAAATTCAGACGA TATTACCTTGCGAAGCTTTTCAA TTCAATTCATCATTT	ATATAATATGAACCTTCAACTA GTTATTACCACTGTGGCACTCT TTCTGCGGTAAGATTATCTCAG GGTAATAACTGATATAATTAAA TT
Fusing $tRNA^{Arg}_{CCU}$ gene variants with *URA3*	CGAAGTTTATTCATTCAATTTGA AG	ATATAATATGAACCTTCAACTA GTTA
First round of PCR for library preparation	GGGGTTCATTACAGCAGCTT	TGTGCTCCTTCCTTCGTTCT
Second round of PCR for library preparation*	AATGATACGGCGACCACCGAG ATCTACACTCTTTCCCTACACG ACGCTCTTCCGATCTNNNNNNA GTTCAACCAAGTTGG	CAAGCAGAAGACGGCATACGA GATCGTGATGTGACTGGAGTT CAGACGTGTGCTCTTCCGATC TAAAAAAAAATAATCAACG

*The underlined sequence in the reverse primer at the second round of PCR corresponds to the index sequence for multiplex sequencing.

Table S2. Illumina read numbers from each sample

Time (hrs)	Sample description	Raw read number	Read pair number after filtering	Percentage used
0	Repeat 1	174,956,172	74,749,170	0.854
	Repeat 2	113,885,948	43,808,386	0.769
24	Replicate 1	45,821,636	19,957,042	0.871
	Replicate 2	29,756,408	12,921,113	0.868
	Replicate 3	51,889,890	22,273,492	0.858
	Replicate 4	119,335,654	53,881,470	0.903
	Replicate 5	67,091,400	29,939,362	0.892
	Replicate 6	82,746,144	37,263,697	0.901

Table S3. Fitness of mutants carrying anticodon mutations

Anticodon	Corresponding codon (by Watson-Crick pairing)	Corresponding amino acid	Fitness
CCC	GGG	G	0.82
ACT	AGT	S	0.80
AGT	ACT	T	0.76
GCT	AGC	S	0.74
CCA	TGG	W	0.71
CAT	ATG	M	0.71
CTT	AAG	K	0.71
TCT	AGA	R	0.69
CCG	CGG	R	0.68
CGT	ACG	T	0.65
TGT	ACA	T	0.65
AAT	ATT	I	0.62
CGC	GCG	A	0.61
CTC	GAG	E	0.61
GCC	GGC	G	0.60
TCC	GGA	G	0.58
TAT	ATA	I	0.57
GTT	AAC	N	0.56
CAC	GTG	V	0.52
ATT	AAT	N	0.50
GGT	ACC	T	0.50
ACC	GGT	G	0.50
GCA	TGC	C	0.50
CTG	CAG	Q	0.50
TCA	TGA	Stop	0.50
CTA	TAG	Stop	0.50

Table S4. Examples of pairwise epistasis whose sign depends on the genetic background

Mut C	Mut A	Mut B	f_C	f_A	f_B	f_{AC}	f_{BC}	f_{AB}	f_{ABC}	$\varepsilon_{AB}\|WT$	$\varepsilon_{AB}\|C$
A15T	G50A	C55G	0.88	1.00	0.70	0.60	0.51	0.71	0.67	-0.18	0.25
G18C	G12A	C29T	0.66	1.00	0.99	0.59	0.55	0.74	0.60	-0.25	0.16
A36C	C27T	G68C	0.70	1.00	0.97	0.54	0.59	0.76	0.60	-0.21	0.21
C33G	A15T	G50A	0.74	0.88	1.00	0.55	0.61	0.71	0.62	-0.18	0.23
C60G	G9C	G67A	0.66	0.85	0.95	0.53	0.58	0.58	0.57	-0.23	0.16
A15C	C5G	C22A	0.90	0.99	1.00	0.63	0.70	0.77	0.63	-0.23	0.16
C33G	A15T	C62G	0.74	0.88	0.92	0.55	0.60	0.65	0.60	-0.17	0.22
A36C	C30T	A65C	0.70	1.01	1.01	0.57	0.60	0.84	0.62	-0.19	0.19
A14C	T7C	G63C	0.87	1.01	0.81	0.68	0.54	0.61	0.57	-0.20	0.16
G48C	C49T	C55T	0.98	1.00	0.72	0.67	0.65	0.79	0.66	-0.18	0.18
C31A	A15T	C49G	0.85	0.88	0.99	0.59	0.64	0.67	0.58	-0.20	0.16
A15T	T16A	C27G	0.88	0.99	0.64	0.53	0.55	0.70	0.59	-0.17	0.17
C31G	G9C	C30T	0.94	0.85	1.01	0.63	0.66	0.79	0.63	-0.16	0.17
A14C	C4G	G48C	0.87	1.01	0.98	0.57	0.66	0.82	0.58	-0.16	0.17
C62G	A20T	G63C	0.92	0.99	0.81	0.68	0.59	0.65	0.60	-0.15	0.15
A40T	A14G	G58C	0.99	0.80	0.99	0.90	0.94	0.99	0.71	0.20	-0.16
C49T	C34T	A65C	1.00	0.71	1.01	0.87	0.94	0.88	0.61	0.17	-0.20
G39A	C5T	C55T	0.99	0.99	0.72	0.94	0.87	0.86	0.61	0.15	-0.22
C49G	C46G	C62A	0.99	0.99	0.72	0.97	0.84	0.87	0.61	0.16	-0.22
G44A	C5T	C55T	0.98	0.99	0.72	1.08	0.78	0.86	0.63	0.15	-0.23
T54C	C5A	G44C	0.81	1.00	0.98	0.80	0.72	0.98	0.56	0.18	-0.20
C49G	T19C	G67T	0.99	0.97	0.92	1.14	0.70	1.07	0.60	0.18	-0.21
A20C	A14G	C46G	1.01	0.80	0.99	0.81	1.02	0.99	0.64	0.20	-0.18
A65T	C46T	C49A	0.99	0.99	0.76	0.86	0.88	0.96	0.55	0.21	-0.21
G48C	C4T	G25A	0.98	0.99	0.98	0.90	0.95	1.14	0.62	0.18	-0.26
A42G	A14G	C46G	0.93	0.80	0.99	0.78	0.89	0.99	0.52	0.20	-0.24
C31A	A45T	A70T	0.85	0.99	1.01	0.93	0.92	1.02	0.79	0.18	-0.26
T28A	C5T	G12C	0.89	0.99	0.98	0.82	0.86	1.04	0.55	0.16	-0.28
G50A	T32A	A69T	1.00	0.74	1.03	0.78	1.00	0.96	0.53	0.19	-0.25
G50A	C46G	C62A	1.00	0.99	0.72	1.04	0.88	0.87	0.60	0.16	-0.30
G67A	G48A	G52A	0.95	0.98	0.70	0.98	0.91	0.83	0.65	0.17	-0.30
A65G	A20G	G23A	1.00	1.00	0.74	0.89	0.99	0.91	0.57	0.17	-0.30
C46G	C31T	G63A	0.99	0.99	0.85	0.97	0.80	1.14	0.61	0.30	-0.18
C55T	G9A	C22A	0.72	0.99	1.00	0.92	0.65	0.92	0.63	0.20	-0.28
C55T	C4G	C5T	0.72	1.01	0.99	0.75	0.75	0.86	0.54	0.15	-0.32
G52A	C46A	G63C	0.70	1.00	0.81	0.82	0.65	1.00	0.56	0.18	-0.30
G23A	C29T	C30A	0.74	0.99	1.00	0.79	0.74	0.92	0.56	0.19	-0.31
C46G	T3A	A14G	0.99	1.00	0.80	0.93	0.98	0.99	0.62	0.20	-0.31
A14G	T2C	C5G	0.80	1.00	0.99	0.74	0.86	1.00	0.56	0.21	-0.30

All listed epistasis values are statistically significant (nominal $P < 0.05$, t-test from the six biological replicates).